This article has been accepted for publication in a future issue of this journal, but has not been fully edited. Content may change prior to final publication. Citation information: DOI 10.1109/TVT.2021.3076825, IEEE Transactions on Vehicular Technology

Energy Efficient Downlink Resource Allocation in Cellular IoT Supported H-CRANs

Lilatul Ferdouse[1], Isaac Woungang[2], Alagan Anpalagan[1], and Serhat Erkucuk[3]
[1]Department of Electrical and Computer Engineering, Ryerson University, Toronto, ON, Canada
[2]Department of Computer Science, Ryerson University, Toronto, ON, Canada
[3]Department of Electrical-Electronics Engineering, Kadir Has University, Istanbul, Turkey

***Abstract*—The cloud computing supported heterogeneous cloud radio access network (H-CRAN) is one of the promising solutions to support cellular IoT devices with the legacy cellular systems. However, the dense deployment of small cells with fractional frequency reuse in orthogonal frequency division multiple access (OFDMA) based H-CRANs increases intra- and inter-cell interference, turning the resource allocation into a more challenging problem. In general, the macro cell users are considered as the legacy users, whereas the cellular IoT devices and small cell users share the macro cell users' resource blocks in an underlaid approach. In this paper, we investigate an underlaid approach of resource allocation for small and macro cell users to improve the energy efficiency (EE) in H-CRANs. The solution approaches are derived with the Dinkelbach, Lagrange and Alternating Direction Method of Multipliers (ADMM) methods by considering maximum power, resource block allocation, fronthaul capacity and quality of service (QoS) constraints of macro cell users. A two-step energy efficient underlaid cellular IoT (UC-IoT) supported H-CRAN method is proposed and evaluated with overlaid cellular IoT (OC-IoT) supported H-CRAN and underlaid H-CRAN without cellular IoT devices. The proposed method is evaluated in terms of energy efficiency and the Jain's fairness index, considering the effect of number of cellular IoT density in each small cell of the H-CRAN. The simulation results demonstrate the effectiveness of the proposed approach compared to earlier approaches.**

Keywords: Energy Efficiency, H-CRAN, OFDMA, Resource Block Allocation, Power Allocation, Cellular IoT Systems.

I. Introduction

The heterogeneous cloud radio access network (H-CRAN) is regarded as an emerging technological and architectural solution for the next generation cellular networks and is expected to handle 100 times more traffic and user loads as well as 1000 times higher network capacity [1]. The H-CRAN consists of remote radio heads (RRHs) in small cells, a centralized baseband unit (BBU) pool and wired/wireless fronthaul links. The fronthaul links connect all RRHs to a BBU pool. The H-CRANs consist of RRHs and macro base stations (MBSs), where RRHs support IoT applications and low data rate users, leaving the network control operations such as interference and handover management, and high data rate users to the macro cell. In addition, all the BBUs in a BBU pool are considered as computing servers to perform baseband signal processing through a cloud computing technology [2]. The integration of computing servers in the BBU pool is considered as a promising solution to handle the computing jobs for smart city applications such as smart healthcare, smart transportation, smart parking, industry automation, etc. [3]. Depending on the application, there are different categories of IoT devices. Among them, some IoT devices are designed in such a way that they use the cellular links for data transmission [4]. For example, in a smart parking system, the cellular IoT device collects all empty slot data and updates the parking information to the cloud so that the users can use

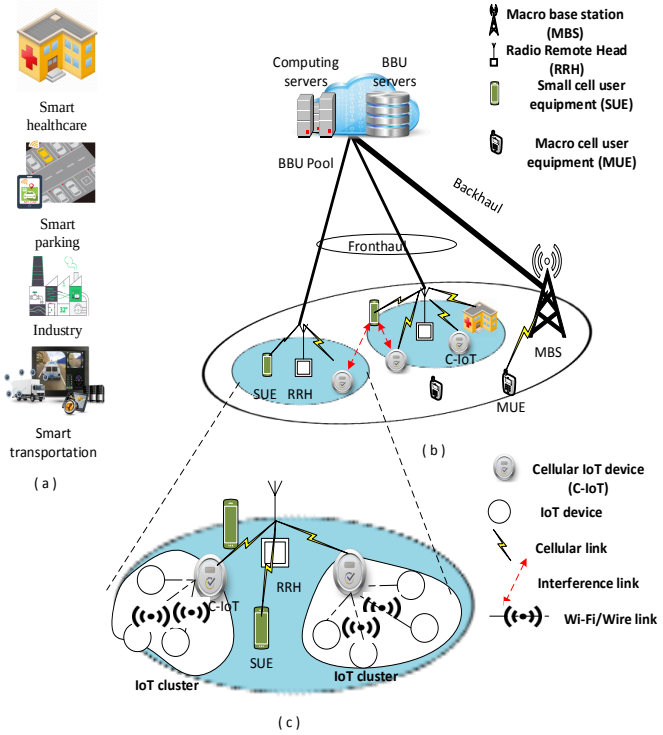

Fig. 1: (a) IoT applications, (b) Cloud computing based heterogeneous cloud radio access network (H-CRAN) with one macro cell and multiple small cells, (c) IoT clusters covered by a small cell, where a cellular IoT device using cellular links may cause interference to other small cell users.

 This work is supported by a grant from the National Science and Engineering Research Council of Canada (NSERC), Reference: RGPIN-2017-04423 and the Ryerson University Faculty of Science Dean's Research Fund, held by the 2nd author.

the cloud data to select the parking spot. Autonomous sensor devices and cellular IoT devices in the industrial IoT (IIoT) systems are managed by the centralized controller. In the cloud computing-based H-CRAN, the BBU pool can maintain computing servers, works as a centralized controller and sends the data to the cellular IoT to operate the IIoT systems. In cloud computing-based cellular IoT supported H-CRAN systems, the cellular IoT device can send/receive data to/from the computing servers in the BBU pool through the RRHs. The cellular IoT devices are referred to as IoT cluster heads or IoT data aggregators [5], which receive data from the other nodes of the IoT cluster. In the downlink communication, the cellular IoT devices receive data from the BBU pool through the RRH and distribute that data to the IoT clusters. The IoT cluster formation and cluster head selection are considered in [5], whereas the design of different data aggregators are discussed in [6]. In this work, we consider a dynamic resource allocation policy among macro, small cell users and cellular-IoT devices to avoid intra- and inter-cell interference in a cellular-IoT supported H-CRAN system.

Deploying a large number of RRHs in a H-CRAN to support cellular IoT devices and improve the network capacity and spectrum efficiency of the next generation cellular networks is a challenging problem [7], [8]. Moreover, the dense deployment of RRHs in a H-CRAN increases the intra- and inter-cell interference. Therefore, dynamic resource allocation and scheduling policy are essential to control the interference level as well as to improve the energy efficiency (EE) and spectrum efficiency (SE) in the cellular IoT supported H-CRAN systems. In this paper, we consider the macro cell users to be the legacy users, which use dedicated orthogonal radio resources, where the small cell users and cellular IoT devices share the same radio resources of macro cell users in an underlaid approach. The underlaid approach of resource allocation supports two or more users that can share the same resource under a dynamic resource allocation policy (i.e., power control, radio resource management), where secondary users cannot interfere with the primary user's communication [9]. The underlaid approach is applied to wireless communication when the number of radio resources is limited and the user density is high. In this paper, the small cell users and cellular IoT devices are considered as secondary users and macro cell users are considered as primary users. Also, a resource scheduling policy is designed to share the same radio resources among the small cell users and cellular IoT devices so that if any macro cell radio resource is not used by small cell users, the cellular IoT devices can utilize those resources for data transmission. We consider the downlink communication, where computing servers from BBU pool send data to the cellular IoTs through cellular links. The energy efficiency aspect of communication resource sharing in a cellular-IoT supported H-CRAN is investigated here.

A. Related work

Considering the EE of H-CRANs, the authors in [10] have proposed an optimal base station sleeping method in a cloud-edge supported H-CRAN system. Authors in [11] have considered an energy harvesting module for H-CRAN system where all the RRHs are powered by energy harvesting. A mesh adaptive direct search algorithm is proposed to improve the EE of H-CRAN system. Similarly in [8], the authors have proposed an EE framework for H-CRAN considering the fractional frequency reuse in both macro and small cells. Authors in [12] have considered only small cell users to maximize EE in H-CRAN via BBU-offloading. However, the authors in [8] and [12] did not consider different categories of small cell users and an underlaid approach of resource sharing. On the other hand, in [8], only energy savings at the BBU pool side has been considered, which used an iterative process to optimize the power in a BBU pool during the low traffic load by switching off the virtual machines inside the BBU pool.

The orthogonal frequency division multiple access (OFDMA) supported long-term evolution (LTE) and long-term evolution advanced (LTE-A) networks utilize orthogonal resources for the users to mitigate the intra-cell interference. Similarly, OFDMA supported H-CRANs utilize orthogonal resources for the small cell users [12], [13] which do not consider the cellular IoT device as a small cell user. The other challenge involved in OFDMA supported systems is the OFDMA systems supporting limited number of users due to the orthogonal radio resource allocation policy for avoiding the interference. One of the potential solutions is the underlaid approach of resource sharing, which improves the spectrum efficiency of the networks as well as the user density [9]. Considering the interference issues, authors in [13] have proposed an auction-based distributed resource allocation with the aim to improve the data rate of small cell users.

Due to the limited number of orthogonal resources, authors in [9] have considered an underlaid approach of orthogonal resource sharing both for macro cell and small cell users, with the aim to maximize the sum of tolerable interference levels. Similarly, in this paper, we consider an underlaid approach of downlink communication resource allocation for both small cell and macro cell users to improve the EE in a H-CRAN. Different from the above earlier works, we optimize the EE performance of H-CRAN while improving the SE by allocating the same orthogonal resources both for macro and small cell users. Also, we consider cellular IoT devices as one of the categories of small cell users who compete in resource sharing with other small cell users.

B. Contributions and Organization of the paper

This paper considers the downlink communication resources (i.e., resource blocks and power) allocation in cellular IoT supported H-CRANs considering both small cell, cellular IoT devices and macro cell users. In the resource allocation optimization problem, we consider the maximum power, resource block allocation, fronthaul capacity and quality of service (QoS) constraints of macro cell users, with the aim to maximize the EE of H-CRAN. To solve the optimization problem, we relax the original problem by replacing non-convex constraints with convex constraints considering the time-sharing approach of resource allocation, then we transform the fractional objective function into a subtractive linear

form. To support the underlaid approach of resource allocation, we divide the original problem into two sub-problems. A two-step energy efficient underlaid cellular IoT supported H-CRAN (UC-IoT) method (i.e., **Algorithm 1**, **Algorithm 2** and **Algorithm 3**) is proposed. The solution approaches are implemented with the Dinkelbach and Alternating Direction Method of Multipliers (ADMM) methods by allocating the same radio resources to cellular IoTs, small cell and macro cell users. In the first step, we apply the Dinkelbach theorem and Lagrange multiplier method (i.e., **Algorithm 1**) to update the resource allocation policy for all macro cell users. For the EE problem, the Dinkelbach approach is very efficient for solving large scale optimization problems. In our model, a two tier C-IoT supported H-CRAN is considered, where constraints are set according to the underlaid approach of RB allocation, total power, minimum data rate and fronthaul capacity requirements. It is proven that for very large scale instances with up to thousands of constraints and variables, the Dinkelbach approach can yield the optimal solution while other mixed integer non-linear programming (MINLP) solvers such as branch-and-bound, outer-approximation method, would need more computational (i.e., memory, CPU cycles) requirements.

In the second step, using the macro cell users' resource allocation policy, each small cell applies **Algorithm 2** and **Algorithm 3** to obtain the optimal EE solution. **Algorithm 3** utilizes the ADMM method, which returns the optimal power allocation solution of each RRH in H-CRAN. The benefit of using the ADMM method in **Algorithm 3** is that it can solve the EE optimization problem in H-CRAN by breaking it into smaller sub-problems, where each sub-problem is then easily handled by each RRH. The effectiveness of the proposed method is verified through Monte Carlo simulation.

The rest of the paper is organized as follows. In Section II, the system model for resource block and power allocation in cellular IoT supported H-CRAN is presented. The corresponding energy efficient resource allocation optimization problem, objective and constraint sets, and the problem formulation are presented in Section II. The relaxed problem and proposed solution approaches are described in Section III. Section IV provides the simulation results of the proposed method. Finally, Section V concludes the paper.

TABLE I: List of symbols

Symbol	Description
$\mathcal{J}$	Number of small cells/RRHs
j	Indexing for RRH
$\mathcal{I}$	Number of SUEs
i	Indexing for SUE
$\mathcal{D}$	Number of C-IoTs
d	Indexing for C-IoTs
$\mathcal{M}$	Number of C-IoTs
m	Indexing for MUE
$\mathcal{K}$	Total number of H-CRAN users
$\mathcal{R}$	Number of RBs
r	Indexing for RB
$\alpha_{i,j}^{r}$	RB allocation variable for r^{th} RB to j^{th} RRH for SUE i
$\boldsymbol{\alpha} = [\alpha_{i,j}^{r}]_{\mathcal{I}\times\mathcal{J}\times\mathcal{R}}$	Matrix of RB allocation for all SUEs
$\beta_{i,j}^{r}$	RB allocation variable for r^{th} RB to B^{th} MBS for MUE m
$\boldsymbol{\beta} = [\beta_{m,B}^{r}]_{\mathcal{M}\times\mathcal{R}}$	Matrix of RB allocation for all MUEs
$h_{i,j}^{r}$	Channel gain from j^{th} RRH to i^{th} SUE on r^{th} RB
$P_{i,j}^{r}$	Power allocation from j^{th} RRH to SUE i on r^{th} RB
P_j	Static power of j^{th} RRH
$\boldsymbol{P_{\mathcal{I}}} = [P_{i,j}^{r}]_{\mathcal{I}\times\mathcal{J}\times\mathcal{R}}$	Matrix of power allocation for all SUEs
$P_{m,B}^{r}$	Power allocation from MBS to MUE m on r^{th} RB
P_B	Static power of B^{th} MBS
$\boldsymbol{P_{\mathcal{M}}} = [P_{m,B}^{r}]_{\mathcal{M}\times\mathcal{R}}$	Matrix of power allocation for all MUEs
P_j^{max}	Maximum power budget of j^{th} RRH
P_B^{max}	Maximum power budget of MBS
$\gamma_{i,j}^{r}$	SINR of i^{th} SUE connected to j^{th} RRH on r^{th} RB
$\gamma_{m,B}^{r}$	SINR of m^{th} MUE connected to B^{th} MBS on r^{th} RB
ω_0	Additive white Gaussian noise term
σ^2	Noise power

II. System model and Assumptions

A. Cellular IoT supported H-CRAN

In this paper, we consider an OFDMA-based two-tier cellular IoT supported H-CRAN which consists of the cloud computing supported BBU pool, one macro cell and remote radio heads covering small geographical location within the macro cell base station and end users. The end users are small cell user equipments (SUE), cellular-IoT (C-IoT) devices and macro cell user equipment (MUE), as shown in Fig. 1. The H-CRAN user equipments have wireless sensor and radio interfaces, which transmit or receive data through the base station to/from the BBU pool. The users are categorized according to the data rate requirements. The high data rate users are considered as macro users connected to the macro BS and low data rate users are SUEs and C-IoT devices. The C-IoT devices are considered as intelligent devices, sometimes referred to as the cluster head, IoT gateway or data aggregator that utilize the cellular links send/receive data to/from the computing servers in the BBU pool. The IoT cluster formation and cluster header selection are out of the scope of this paper. The BBU pool considers a centralized controller which manages the user association, communication (i.e., spectrum and power) and computing (i.e., BBU servers, computing servers, etc.) resource allocation in the coverage area [2]. Using the control channel, the BBU pool collects the channel state information (CSI), traffic information, users data rate requirement, and available communication resources information. In this work, an energy efficient underlaid resource allocation policy is investigated and implemented for H-CRAN based C-IoT systems that optimizes the network performance by allocating the downlink communication resources to the end users.

B. Network Model

We consider an OFDMA-based two-tier H-CRAN cellular IoT system, as shown in Fig. 1, where $\mathcal{S}$ number of small cells having $\mathcal{J}$ number of RRHs, indexed by $j = \{1, 2, ..., \mathcal{J}\}$, are covered by a single macro cell B with an underlaid approach. For simplicity, we assume that the system supports a total number of $\mathcal{R}$ resource blocks (RB), indexed by $r = \{1, 2, 3, ..., \mathcal{R}\}$ jointly assigned by the BBU pool to all end users. The system supports a total number of users $\mathcal{K} = \mathcal{I} \bigcup \mathcal{D} \bigcup \mathcal{M}$, where SUEs are indexed by $i = \{1, 2, 3, ..., \mathcal{I}\}$, C-IoT devices are indexed by $d = \{1, 2, 3, ..., \mathcal{D}\}$ and MUEs are denoted by $m = \{1, 2, 3, ..., \mathcal{M}\}$. Notation $\alpha_{i,j}^{r}$ denotes the RB allocation between SUE i and RB r on RRH j with $\alpha_{i,j}^{r} = 1$ if RB r is assigned to SUE i in RRH j and otherwise $\alpha_{i,j}^{r} = 0$. Similarly,

This article has been accepted for publication in a future issue of this journal, but has not been fully edited. Content may change prior to final publication. Citation information: DOI 10.1109/TVT.2021.3076825, IEEE Transactions on Vehicular Technology

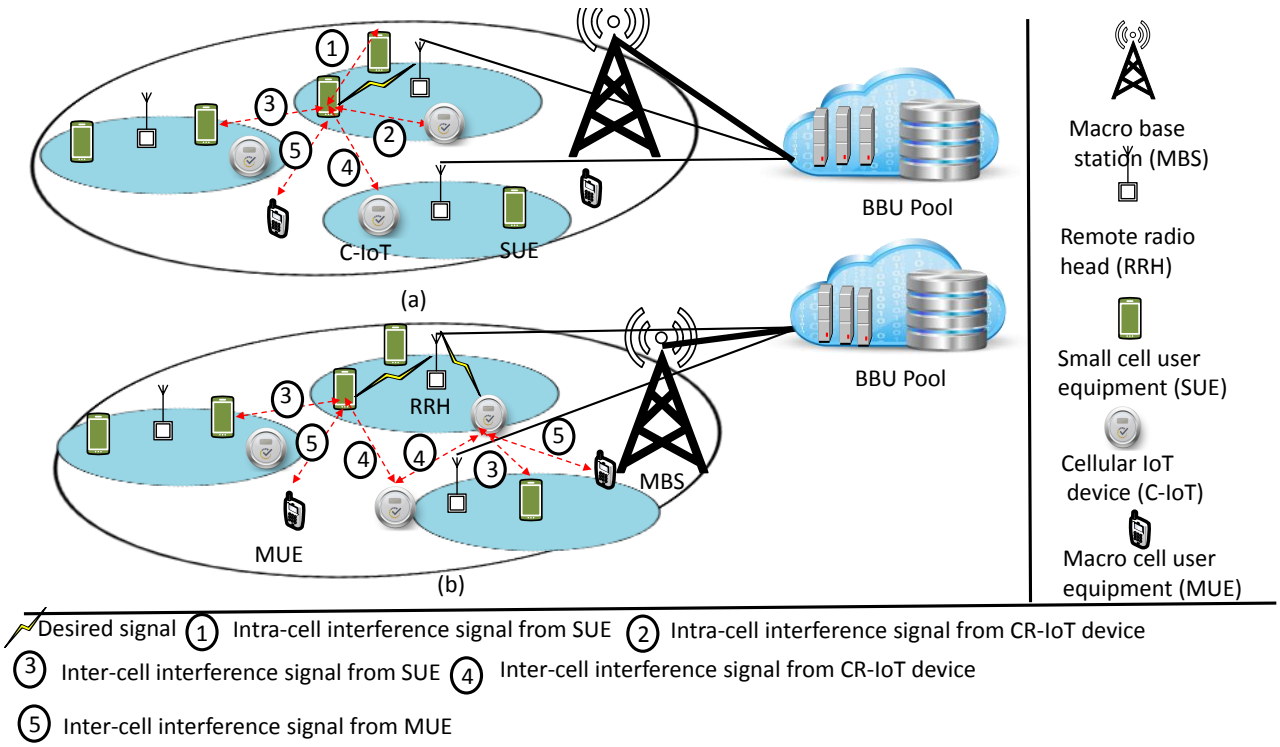

Fig. 2: (a) Without applying the RB and interference mitigation constraints (b) With applying the RB and interference mitigation constraints.

$\rho^r_{d,j} = 1$ denotes the RB allocation between C-IoT device d and RB r on RRH j or otherwise $\rho^r_{d,j} = 0$ and $\beta^r_{m,B} = 1$ indicates that RB r is assigned to MUE m in MBS B.

The channel gain from RRH j to SUE i and C-IoT device d on RB r is denoted as $h^r_{i,j}$ and $h^r_{d,j}$, respectively. The power allocated from RRH j to SUE i and C-IoT device d on RB r is denoted as $P^r_{i,j} \in (0, P^{max}_j]$ and $P^r_{d,j} \in (0, P^{max}_j]$, respectively, where P^{max}_j denotes the maximum power of RRH j. The transmitted data symbol for user i is denoted by x_i, where $\mathrm{E}[|x_i|^2] = 1$. The received signal of SUE i on RB r can be written as:

$$Y^r_i = \underbrace{\left(h^r_{i,j}\alpha^r_{i,j}P^r_{i,j}\right)x_i}_{desired\ signal} + \underbrace{\sum_{k=1,k\neq i}^{\mathcal{I}\bigcup\mathcal{D}}\left(h^r_{i,j}\alpha^r_{k,j}\rho^r_{k,j}P^r_{k,j}\right)x_k}_{interference\ signal\ from\ the\ same\ cell} + \underbrace{\sum_{l=1,l\neq i}^{\mathcal{I}\bigcup\mathcal{D}}\left(\sum_{n=1,n\neq j}^{\mathcal{J}} h^r_{i,n}\alpha^r_{l,n}\rho^r_{l,n}P^r_{l,n}\right)x_l}_{interference\ signal\ from\ other\ small\ cells} + \underbrace{\sum_{m=1}^{\mathcal{M}} h^r_{i,B}\beta^r_{m,B}P^r_{m,B}x_m}_{interference\ signal\ from\ the\ macro\ cell} + \omega_0, \quad (1)$$

where the first term on the right hand side of (1) is the desired signal for user i from RRH j on RB r, the second and third terms denote the interference signal coming from other active SUEs and C-IoT devices of the same and other cells using the same RB r, respectively. The fourth term determines the interference signal from all active MUEs using the same RB r. The term ω_o represents the additive white Gaussian noise, where the noise variance is denoted by σ^2. The signal-to-interference-noise ratio (SINR) achieved by SUE i, attached to RRH j on RB r can be written as

$$\gamma^r_{i,j} = \frac{\alpha^r_{i,j}P^r_{i,j}|h^r_{i,j}|^2}{I^r_{i,j} + \sigma^2}, \quad (2)$$

where $I^r_{i,j}$ represents the aggregated interference power, defined as in [9], [14], i.e.

$$I^r_{i,j} = \underbrace{\sum_{\substack{k=1,\\k\neq i}}^{\mathcal{I}\bigcup\mathcal{D}} \alpha^r_{k,j}\rho^r_{k,j}P^r_{k,j}|h^r_{i,j}|^2}_{intra-cell\ interference\ from\ the\ same\ small\ cell} + \underbrace{\sum_{\substack{l=1,\\l\neq i}}^{\mathcal{I}\bigcup\mathcal{D}}\sum_{\substack{n=1,\\n\neq j}}^{\mathcal{J}} \alpha^r_{l,n}\rho^r_{l,n}P^r_{l,n}|h^r_{i,n}|^2}_{inter-cell\ interference\ from\ all\ small\ cells} + \underbrace{\sum_{m=1}^{\mathcal{M}} \beta^r_{m,B}P^r_{m,B}|h^r_{i,B}|^2}_{inter-cell\ interference\ from\ macro\ cell}. \quad (3)$$

Similarly, the SINR achieved by the C-IoT device d, attached

This article has been accepted for publication in a future issue of this journal, but has not been fully edited. Content may change prior to final publication. Citation information: DOI 10.1109/TVT.2021.3076825, IEEE Transactions on Vehicular Technology

to RRH j on r can be expressed by

$$\gamma_{d,j}^{r} = \frac{\rho_{d,j}^{r} P_{d,j}^{r} |h_{d,j}^{r}|^2}{I_{d,j}^{r} + \sigma^2}, \tag{4}$$

where $I_{d,j}^{r}$ is defined as

$$I_{d,j}^{r} = \underbrace{\sum_{\substack{k=1,\\ k\neq d}}^{\mathcal{I}\bigcup\mathcal{D}} \alpha_{k,j}^{r} \rho_{k,j}^{r} P_{k,j}^{r} |h_{d,j}^{r}|^2}_{intra-cell\ interference\ from\ the\ same\ small\ cell} + \underbrace{\sum_{\substack{l=1,\\ l\neq d}}^{\mathcal{I}\bigcup\mathcal{D}} \sum_{\substack{n=1,\\ n\neq j}}^{\mathcal{J}} \alpha_{l,n}^{r} \rho_{l,n}^{r} P_{l,n}^{r} |h_{d,n}^{r}|^2}_{inter-cell\ interference\ from\ all\ small\ cells} + \underbrace{\sum_{m=1}^{\mathcal{M}} \beta_{m,B}^{r} P_{m,B}^{r} |h_{d,B}^{r}|^2}_{inter-cell\ interference\ from\ macro\ cell} . \tag{5}$$

and the SINR achieved by MUE m, attached to MBS B on r can be expressed by

$$\gamma_{m,B}^{r} = \frac{\beta_{m,B}^{r} P_{m,B}^{r} |h_{m,B}^{r}|^2}{I_{m,B}^{r} + \sigma^2}, \tag{6}$$

where $I_{m,B}^{r}$ represents the aggregated interference power of macro cell user m observed in RB r, which can be expressed as

$$I_{m,B}^{r} = \underbrace{\sum_{k=1,k\neq m}^{\mathcal{M}} \beta_{k,B}^{r} P_{k,B}^{r} |h_{m,B}^{r}|^2}_{intra-cell\ interference\ from\ other\ macro\ cell\ users} + \underbrace{\sum_{l=1,l\neq m}^{\mathcal{I}\bigcup\mathcal{D}} \sum_{j=1}^{\mathcal{J}} \alpha_{l,j}^{r} \rho_{l,j}^{r} P_{l,j}^{r} |h_{m,j}^{r}|^2}_{inter-cell\ interference\ from\ all\ small\ cells} . \tag{7}$$

C. Problem Formulation

According to the Shannon theory, the achievable data rate by SUE i and C-IoT device d from SBS j on RB r are $R_{i,j}^{r} = \triangle f \log_2(1+\gamma_{i,j}^{r})$ and $R_{d,j}^{r} = \triangle f \log_2(1+\gamma_{d,j}^{r})$ respectively, where $\triangle f$ denotes the bandwidth allocated to each RB, and the total data rate of all SUEs can be expressed as

$$R_{T_s}(\boldsymbol{\alpha}, \boldsymbol{P_{\mathcal{I}}}) = \sum_{i=1}^{\mathcal{I}} \sum_{j=1}^{\mathcal{J}} \sum_{r=1}^{\mathcal{R}} \alpha_{i,j}^{r} R_{i,j}^{r}. \tag{8}$$

Similarly, the achievable data rate of all C-IoT devices and macro cell users can be expressed as:

$$R_{T_d}(\boldsymbol{\rho}, \boldsymbol{P_{\mathcal{D}}}) = \sum_{d=1}^{\mathcal{D}} \sum_{j=1}^{\mathcal{J}} \sum_{r=1}^{\mathcal{R}} \rho_{d,j}^{r} R_{d,j}^{r} \tag{9}$$

and

$$R_{T_m}(\boldsymbol{\beta}, \boldsymbol{P_{\mathcal{M}}}) = \sum_{m=1}^{\mathcal{M}} \sum_{r=1}^{\mathcal{R}} \beta_{m,B}^{r} R_{m,B}^{r}, \tag{10}$$

respectively. The total allocated powers of small and macro cell users are denoted by

$$P_{T_j}(\boldsymbol{\alpha}, \boldsymbol{P_{\mathcal{I}}}) = \underbrace{\sum_{i=1}^{\mathcal{I}} \sum_{j=1}^{\mathcal{J}} \sum_{r=1}^{\mathcal{R}} \alpha_{i,j}^{r} P_{i,j}^{r}}_{dynamic} + \underbrace{\sum_{j=1}^{\mathcal{J}} P_j}_{static}, \tag{11}$$

and

$$P_{T_B}(\boldsymbol{\beta}, \boldsymbol{P_{\mathcal{M}}}) = \underbrace{\sum_{m=1}^{\mathcal{M}} \sum_{r=1}^{\mathcal{R}} \beta_{m,B}^{r} P_{m,B}^{r}}_{dynamic} + \underbrace{P_B}_{static}, \tag{12}$$

respectively. Similar to [15], we assume that each small and macro cell has dynamic and static power factors. The dynamic power depends on the resource allocation, whereas the alternative current (AC) circuit power is regarded as static power. The total power of C-IoT device depends on the transmission power and device activation, sensing and reception (ASR) power [5].

$$P_{T_d}(\boldsymbol{\rho}, \boldsymbol{P_{\mathcal{D}}}) = \underbrace{\sum_{d=1}^{\mathcal{D}} \sum_{j=1}^{\mathcal{J}} \sum_{r=1}^{\mathcal{R}} \rho_{d,j}^{r} P_{d,j}^{r}}_{Transmission} + \underbrace{\sum_{d=1}^{\mathcal{D}} P_d}_{ASR}, \tag{13}$$

The objective of the resource allocation is to maximize the EE (i.e., η) in terms of data rate and power. The EE can be measured by the ratio of total achievable data rate and total allocated power (bits/W), written as:

$$\begin{aligned} \eta &= \frac{R_{T_j}(\boldsymbol{\alpha}, \boldsymbol{P_{\mathcal{I}}}) + R_{T_d}(\boldsymbol{\rho}, \boldsymbol{P_{\mathcal{D}}}) + R_{T_m}(\boldsymbol{\beta}, \boldsymbol{P_{\mathcal{M}}})}{P_{T_j}(\boldsymbol{\alpha}, \boldsymbol{P_{\mathcal{I}}}) + P_{T_d}(\boldsymbol{\rho}, \boldsymbol{P_{\mathcal{D}}}) + P_{T_B}(\boldsymbol{\beta}, \boldsymbol{P_{\mathcal{M}}})}, \\ &= \frac{R_T(\boldsymbol{\alpha}, \boldsymbol{\rho}, \boldsymbol{\beta}, \boldsymbol{P_{\mathcal{I}}}, \boldsymbol{P_{\mathcal{D}}}, \boldsymbol{P_{\mathcal{M}}})}{P_T(\boldsymbol{\alpha}, \boldsymbol{\rho}, \boldsymbol{\beta}, \boldsymbol{P_{\mathcal{I}}}, \boldsymbol{P_{\mathcal{D}}}, \boldsymbol{P_{\mathcal{M}}})} \end{aligned} \tag{14}$$

where $\boldsymbol{\alpha}, \boldsymbol{\rho}, \boldsymbol{\beta}, \boldsymbol{P_{\mathcal{I}}}, \boldsymbol{P_{\mathcal{D}}}$, and $\boldsymbol{P_{\mathcal{M}}}$ are the RB association and power allocation policies for all SUEs, C-IoT devices and MUEs, respectively.

We define the following constraint sets in order to maximize the EE in a H-CRAN based C-IoT system. In the constraint sets, we consider that all users are associated with either the RRHs or the MBS, utilizing the RBs and power to transmit the data without causing interference to each other.

RB association and interference mitigation constraints:

$$\text{C1:} \quad \sum_{r=1}^{\mathcal{R}} \beta_{m,B}^{r} \leq 1, \quad \forall m \in \mathcal{M}, \tag{15}$$

$$\text{C2:} \quad \sum_{r=1}^{\mathcal{R}} \beta_{m,B}^{r} (\alpha_{i,j}^{r} + \rho_{d,j}^{r}) \leq 1, \quad \forall i \in \mathcal{I}, \forall d \in \mathcal{D}, \forall j \in \mathcal{J}, \tag{16}$$

$$\text{C3:} \quad \beta_{m,B}^{r} \in \{0,1\}, \quad \alpha_{i,j}^{r} \in \{0,1\}, \quad \rho_{d,j}^{r} \in \{0,1\}. \tag{17}$$

Constraint **C1** ensures that each RB is associated with only one MUE. However, for spectrum efficiency we assume

that an SUE or a C-IoT device can utilize the MUE's RB in an underlaid approach. The underlaid approach of RB allocation increases the intra- and inter-cell interference levels in H-CRAN as shown in Fig. 2(a). To mitigate the intra-cell interference, we incorporate constraint **C2** which ensures that each MUE RB is associated with only one SUE or C-IoT in each small cell. Constraint **C3** enforces the binary association of RB. Fig. 2(b) shows the scenario after applying the **C2** and **C3** constraints. For the inter-cell interference, we assume that the centralized BBU pool manages the interference level among the RRHs.

Maximum power constraint: In this work, we consider the downlink transmission, where the end users get data from the BBU pool from a base station. The C-IoT devices receive instructions through the cellular links from the RRHs. For downlink transmission, we consider the maximum power budget of the base station that is allocated to the transmission links. The constraint **C4** ensures the upper limit of the transmission power of each RRH which is allocated to the transmission links of SUEs and C-IoT devices. Similarly, constraint **C5** ensures the maximum power budget of MBS which is distributed among the transmission links between MBS and MUEs.

$$\text{C4:} \quad \sum_{i=1}^{\mathcal{I}}\sum_{r=1}^{\mathcal{R}} \alpha_{i,j}^{r} P_{i,j}^{r} + \sum_{d=1}^{\mathcal{D}}\sum_{r=1}^{\mathcal{R}} \rho_{d,j}^{r} P_{d,j}^{r} \leq P_{j}^{max}, \quad \forall j \in \mathcal{J}, \tag{18}$$

$$\text{C5:} \quad \sum_{m=1}^{\mathcal{M}}\sum_{r=1}^{\mathcal{R}} \beta_{m,B}^{r} P_{m,B}^{r} \leq P_{B}^{max}. \tag{19}$$

Minimum data rate constraint: As the SUE and the C-IoT device share the same RB with the MUE, the minimum rate constraint ensures the QoS of MUE in **C6** as

$$\text{C6:} \quad \sum_{r=1}^{\mathcal{R}} \beta_{m,B}^{r} R_{m,B}^{r} \geq R_{min}, \quad \forall m \in \mathcal{M}, \tag{20}$$

where R_{min} is the minimum data rate threshold value for MUE.

Fronthaul capacity constraint: Constraint **C7** ensures the maximum fronthaul capacity of each RRH, where F_j^{max} refers to the maximum limit of the signals transmitted on the fronthaul link of each RRH, and it is given as

$$\text{C7:} \quad \sum_{i=1}^{\mathcal{I}}\sum_{r=1}^{\mathcal{R}} \alpha_{i,j}^{r} + \sum_{d=1}^{\mathcal{D}}\sum_{r=1}^{\mathcal{R}} \rho_{d,j}^{r} \leq F_{j}^{max}, \quad \forall j \in \mathcal{J}. \tag{21}$$

The mathematical formulation of the energy efficient resource allocation problem can be described as follows:

$$\text{P1:} \max_{\boldsymbol{\alpha},\boldsymbol{\rho},\boldsymbol{\beta},\boldsymbol{P_{\mathcal{I}}},\boldsymbol{P_{\mathcal{D}}},\boldsymbol{P_{\mathcal{M}}}} \eta \tag{22}$$
$$\text{subject to: C1-C7}$$

In (22), the objective is to maximize the EE of the H-CRAN system by allocating the macro cell users' radio resources to small cell users and C-IoT devices considering the quality of service constraint of macro cell users. The optimization parameters considered in this problem are : i) RB allocation for SUEs, CR-IoT devices and MUEs (i.e., $\alpha_{i,j}^{r} \in \{0,1\}$,$\rho_{d,j}^{r} \in \{0,1\}$, $\beta_{m,B}^{r} \in \{0,1\}$ and ii) power allocation for end users (i.e., $P_{i,j}^{r}$, $P_{d,j}^{r}$ and $P_{m,B}^{r}$).

III. Solution Approaches

The objective function in (22) and the constraint **C3** turn the problem **P1** into a mixed integer non-convex fractional programming problem. The optimization problem **P1** is computationally intractable and is an NP-hard problem [16], [17]. Therefore, we relax the problem **P1** by replacing the non-convex constraints with the convex constraints and transform the fractional objective function of **P1** to the subtractive linear form. First, we relax the constraint **C3** by assuming the time sharing approach of the RB allocation [18], i.e., $0 \leq \alpha_{i,j}^{r} \leq 1$, $0 \leq \rho_{d,j}^{r} \leq 1$, and $0 \leq \beta_{m,B}^{r} \leq 1$. We introduce three new variables $\Gamma_{i,j}^{r} = \alpha_{i,j}^{r} \in (0,1]$ and $\Theta_{d,j}^{r} = \rho_{d,j}^{r} \in (0,1]$ and $\Lambda_{m,B}^{r} = \beta_{m,B}^{r} \in (0,1]$. $\Gamma_{i,j}^{r}$, $\Theta_{d,j}^{r}$ and $\Lambda_{m,B}^{r}$ represent the time sharing factors of the resource blocks of SUE, C-IoT device and MUE, respectively. It denotes the portion of time the RB r is allocated to the user. Let $\mathcal{P}_{\mathcal{I}}{}_{i,j}^{r} = \Gamma_{i,j}^{r} \times P_{i,j}^{r}$, $\mathcal{P}_{\mathcal{D}}{}_{d,j}^{r} = \Theta_{d,j}^{r} \times P_{d,j}^{r}$ and $\mathcal{P}_{\mathcal{M}}{}_{m,B}^{r} = \Lambda_{m,B}^{r} \times P_{m,B}^{r}$, where $\mathcal{P}_{\mathcal{I}}{}_{i,j}^{r}$, $\mathcal{P}_{\mathcal{D}}{}_{d,j}^{r}$ denote the actual transmit power of the SUE i and C-IoT device d on RB r respectively. $\mathcal{P}_{\mathcal{M}}{}_{m,B}^{r}$ is the allocated power of MUE m on RB r. Next, according to [8] and [15], we can transform the fractional objective function of **P1** to the subtractive linear form. The relaxed problem can be represented by:

$$\text{P2:} \max_{\boldsymbol{\Gamma},\boldsymbol{\Theta},\boldsymbol{\Lambda},\boldsymbol{P_{\mathcal{I}}},\boldsymbol{P_{\mathcal{D}}},\boldsymbol{P_{\mathcal{M}}}} R_T(\boldsymbol{\Gamma},\boldsymbol{\Theta},\boldsymbol{\Lambda},\boldsymbol{P_{\mathcal{I}}},\boldsymbol{P_{\mathcal{D}}},\boldsymbol{P_{\mathcal{M}}}) - q^{*} P_T(\boldsymbol{\Gamma},\boldsymbol{\Theta},\boldsymbol{\Lambda},\boldsymbol{P_{\mathcal{I}}},\boldsymbol{P_{\mathcal{D}}},\boldsymbol{P_{\mathcal{M}}})$$
$$\text{subject to:} \tag{23}$$

$$\vec{\text{C1}}: \quad \sum_{r=1}^{\mathcal{R}} \Lambda_{m,B}^{r} \leq 1, \quad \forall m \in \mathcal{M},$$

$$\vec{\text{C2}}: \quad \sum_{r=1}^{\mathcal{R}} \Lambda_{m,B}^{r} (\Gamma_{i,j}^{r} + \Theta_{d,j}^{r}) \leq 1, \quad \forall i \in \mathcal{I}, \forall d \in \mathcal{D}, \forall j \in \mathcal{J},$$

$$\vec{\text{C3}}: \quad \Lambda_{m,B}^{r} \in (0,1], \quad \Gamma_{i,j}^{r} \in (0,1], \quad \Theta_{d,j}^{r} \in (0,1],$$

$$\vec{\text{C4}}: \quad \sum_{i=1}^{\mathcal{I}}\sum_{r=1}^{\mathcal{R}} \mathcal{P}_{\mathcal{I}}{}_{i,j}^{r} + \sum_{d=1}^{\mathcal{D}}\sum_{r=1}^{\mathcal{R}} \mathcal{P}_{\mathcal{D}}{}_{d,j}^{r} \leq P_{j}^{max}, \quad \forall j \in \mathcal{J},$$

$$\vec{\text{C5}}: \quad \sum_{m=1}^{\mathcal{M}}\sum_{r=1}^{\mathcal{R}} \mathcal{P}_{\mathcal{M}}{}_{m,B}^{r} \leq P_{B}^{max}.$$

$$\vec{\text{C6}}: \quad \sum_{r=1}^{\mathcal{R}} \Lambda_{m,B}^{r} R_{m,B}^{r} \geq R_{min}, \quad \forall m \in \mathcal{M},$$

$$\vec{\text{C7}}: \quad \sum_{i=1}^{\mathcal{I}}\sum_{r=1}^{\mathcal{R}} \Gamma_{i,j}^{r} + \sum_{d=1}^{\mathcal{D}}\sum_{r=1}^{\mathcal{R}} \Theta_{d,j}^{r} \leq F_{j}^{max}, \quad \forall j \in \mathcal{J}.$$

where q^{*} is the global optimal EE, i.e.,

$$q^{*} = \frac{R_T(\boldsymbol{\Gamma}^{*},\boldsymbol{\Theta}^{*},\boldsymbol{\Lambda}^{*},\boldsymbol{P_{\mathcal{I}}^{*}},\boldsymbol{P_{\mathcal{D}}^{*}},\boldsymbol{P_{\mathcal{M}}^{*}})}{P_T(\boldsymbol{\Gamma}^{*},\boldsymbol{\Theta}^{*},\boldsymbol{\Lambda}^{*},\boldsymbol{P_{\mathcal{I}}^{*}},\boldsymbol{P_{\mathcal{D}}^{*}},\boldsymbol{P_{\mathcal{M}}^{*}})} = \max_{\boldsymbol{\Gamma},\boldsymbol{\Theta},\boldsymbol{\Lambda},\boldsymbol{P_{\mathcal{I}}},\boldsymbol{P_{\mathcal{D}}},\boldsymbol{P_{\mathcal{M}}}} \frac{R_T(\boldsymbol{\Gamma},\boldsymbol{\Theta},\boldsymbol{\Lambda},\boldsymbol{P_{\mathcal{I}}},\boldsymbol{P_{\mathcal{D}}},\boldsymbol{P_{\mathcal{M}}})}{P_T(\boldsymbol{\Gamma},\boldsymbol{\Theta},\boldsymbol{\Lambda},\boldsymbol{P_{\mathcal{I}}},\boldsymbol{P_{\mathcal{D}}},\boldsymbol{P_{\mathcal{M}}})}. \tag{24}$$

The objective function in (23) is concave, the constraint ($\vec{\mathbf{C6}}$) is convex and the remaining constraints in ($\vec{\mathbf{C1}}$)-($\vec{\mathbf{C5}}$), ($\vec{\mathbf{C7}}$) are affine. Therefore, the optimization problem **P2** is convex [17]. The relaxed problem **P2** satisfies the time-sharing approach of RB allocation. In [19], the authors showed that the duality gap is negligible when the time-sharing condition is satisfied. Therefore, when the number of RBs is sufficiently large, the solution of the relaxed problem is asymptotically optimal.

The global optimal solution q^* in (23) and (24) is difficult to achieve because an underlaid approach of RB allocation scheduling polices is assumed in the system model. The RB and power allocation policy for MUEs (i.e. $\boldsymbol{\Lambda}, \boldsymbol{P_{\mathcal{M}}}$) needs to be derived first. Then, using the MUEs resource allocation information ($\boldsymbol{\Lambda}, \boldsymbol{P_{\mathcal{M}}}$), the feasible resource allocation solution for SUEs and C-IoTs will be derived. Therefore, we have adopted a two-step iterative approach to solve the problem **P2**. We have split **P2** into two sub-problems: i) resource allocation for MUEs (**P3**) and ii) resource allocation for SUEs and C-IoT devices (**P4**). The resource allocation problem for MUEs can be formulated as

$$\begin{aligned}
&\text{P3:} \max_{\boldsymbol{\Lambda}, \boldsymbol{P_{\mathcal{M}}}} R_T(\boldsymbol{\Lambda}, \boldsymbol{P_{\mathcal{M}}}) - u^*\big(P_T(\boldsymbol{\Lambda}, \boldsymbol{P_{\mathcal{M}}})\big) \\
&\quad \text{subject to:} \qquad (25)\\
&\vec{\text{C1}}: \quad \sum_{r=1}^{\mathcal{R}} \Lambda_{m,B}^r \le 1, \quad \forall m \in \mathcal{M}, \\
&\vec{\text{C3}}: \quad \Lambda_{m,B}^r \in (0,1], \\
&\vec{\text{C5}}: \quad \sum_{m=1}^{\mathcal{M}} \sum_{r=1}^{\mathcal{R}} \mathcal{P}_{\mathcal{M}}{}_{m,B}^{r} \le P_B^{max}. \\
&\vec{\text{C6}}: \quad \sum_{r=1}^{\mathcal{R}} \Lambda_{m,B}^r R_{m,B}^r \ge R_{min}, \quad \forall m \in \mathcal{M}.
\end{aligned}$$

where u^* is the optimal EE solution for MUEs, i.e.,

$$u^* = \frac{R_T(\boldsymbol{\Lambda^*}, \boldsymbol{P_{\mathcal{M}}^*})}{P_T(\boldsymbol{\Lambda^*}, \boldsymbol{P_{\mathcal{M}}^*})} = \max_{\boldsymbol{\Lambda}, \boldsymbol{P_{\mathcal{M}}}} \frac{R_T(\boldsymbol{\Lambda}, \boldsymbol{P_{\mathcal{M}}})}{P_T(\boldsymbol{\Lambda}, \boldsymbol{P_{\mathcal{M}}})}.$$

Theorem 1: *For* $R_T(\boldsymbol{\Lambda^*}, \boldsymbol{P_{\mathcal{M}}^*}) \ge 0$ *and* $P_T(\boldsymbol{\Lambda^*}, \boldsymbol{P_{\mathcal{M}}^*}) > 0$, u *can reach its optimal value if and only if*

$$\max_{\boldsymbol{\Lambda}, \boldsymbol{P_{\mathcal{M}}}} R_T(\boldsymbol{\Lambda}, \boldsymbol{P_{\mathcal{M}}}) - u^* P_T(\boldsymbol{\Lambda}, \boldsymbol{P_{\mathcal{M}}}) = 0$$

Proof: See **Appendix A**.

Similarly, the RBs and power optimization problem for SUEs and C-IoTs can be formulated as

$$\begin{aligned}
&\text{P4:} \max_{\boldsymbol{\Gamma}, \boldsymbol{\Theta}, \boldsymbol{P_{\mathcal{I}}}, \boldsymbol{P_{\mathcal{D}}}} R_T(\boldsymbol{\Gamma}, \boldsymbol{\Theta}, \boldsymbol{P_{\mathcal{I}}}, \boldsymbol{P_{\mathcal{D}}}) - v^* P_T(\boldsymbol{\Gamma}, \boldsymbol{\Theta}, \boldsymbol{P_{\mathcal{I}}}, \boldsymbol{P_{\mathcal{D}}}) \\
&\quad \text{subject to:} \qquad (26)\\
&\vec{\text{C2}}: \quad \sum_{r=1}^{\mathcal{R}} \Lambda_{m,B}^r (\Gamma_{i,j}^r + \Theta_{d,j}^r) \le 1, \quad \forall i \in \mathcal{I}, \forall d \in \mathcal{D}, \forall j \in \mathcal{J}, \\
&\vec{\text{C3}}: \quad \Gamma_{i,j}^r \in (0,1], \quad \Theta_{d,j}^r \in (0,1], \\
&\vec{\text{C4}}: \quad \sum_{i=1}^{\mathcal{I}} \sum_{r=1}^{\mathcal{R}} \mathcal{P}_{\mathcal{I}}{}_{i,j}^{r} + \sum_{d=1}^{\mathcal{D}} \sum_{r=1}^{\mathcal{R}} \mathcal{P}_{\mathcal{D}}{}_{d,j}^{r} \le P_j^{max}, \quad \forall j \in \mathcal{J}, \\
&\vec{\text{C6}}: \quad \sum_{r=1}^{\mathcal{R}} \Lambda_{m,B}^r R_{m,B}^r \ge R_{min}, \quad \forall m \in \mathcal{M}. \\
&\vec{\text{C7}}: \quad \sum_{i=1}^{\mathcal{I}} \sum_{r=1}^{\mathcal{R}} \Gamma_{i,j}^r + \sum_{d=1}^{\mathcal{D}} \sum_{r=1}^{\mathcal{R}} \Theta_{d,j}^r \le F_j^{max}, \quad \forall j \in \mathcal{J}.
\end{aligned}$$

A. Resource Allocation Policy for MUEs

To perform the power allocation of MUE, we use the Karush-Kuhn-Tucker (KKT) optimality and define the Lagrangian function in (27), which is given at the top of the next page. In (27), $\delta^{\mathcal{M}}, \zeta_m^{\mathcal{M}}$ are the Lagrange multipliers for the constraints C5 and C6 of problem **P3**, respectively. Differentiating (27) with respect to $P_{m,B}^r$, we obtain the following power allocation of MUE m over RB r as

$$P_{m,B}^r = \left[\frac{1 - \eta_m^{\mathcal{M}}}{\ln(u - \delta^{\mathcal{M}})} - \frac{1}{G_{m,B}^r} \right]^+, \qquad (28)$$

where $G_{m,B}^r = \frac{|h_{m,B}^r|^2}{I_{m,B}^r + \sigma^2}$ and $[\varepsilon]^+ = \max(\varepsilon, 0)$, which is a multi-level water filling allocation [17]. The calculation of (28) is provided in **Appendix B.**

Knowing $P_{m,B}^r$ and u, we can get the RB for MUE by taking the derivative of (27) with respect to $\Lambda_{m,B}^r$

$$\frac{\partial \mathbb{L}}{\partial \Lambda_{m,B}^r} = \Delta_m^r \begin{cases} < 0, & \Lambda_{m,B}^r = 0 \\ = 0, & 0 < \Lambda_{m,B}^r < 1 \\ > 0, & \Lambda_{m,B}^r = 1 \end{cases} \qquad (29)$$

where $\Delta_m^r = (1 - \zeta_m^{\mathcal{M}}) \log_2(1 + \gamma_{m,B}^r) + P_{m,B}^r (u - \delta^{\mathcal{M}})$. (29) shows the three KKT conditions for the RB allocation to the MUE. The Δ_m^r will be positive when $\Lambda_{m,B}^r = 1$ and the RB r^* is allocated to the MUE m with the largest $\Delta_{m,B}^r$, i.e.

$$\Lambda_{m,B}^{r^*} = 1 \text{ when } r^* = \max \Delta_m^r \forall r \qquad (30)$$

For the variable update, the following equations are used:

$$\delta^{\mathcal{M}}(t+1) = \delta^{\mathcal{M}}(t) - \xi_1^t \left\{ P_B^{max} - \sum_{m=1}^{\mathcal{M}} \sum_{r=1}^{\mathcal{R}} \Lambda_{m,B}^r P_{m,B}^r \right\} \qquad (31)$$

$$\zeta_m^{\mathcal{M}}(t+1) = \zeta_m^{\mathcal{M}}(t) - \xi_2^t \left\{ \sum_{m=1}^{\mathcal{M}} \sum_{r=1}^{\mathcal{R}} \left\{ \Lambda_{m,B}^r \log_2(1 + \gamma_{m,B}^r) - R_{min} \right\} \right\} \qquad (32)$$

The iterative approaches to obtain the optimal EE u^* and resource allocation policy (i.e., $(\boldsymbol{\Lambda}, \boldsymbol{P_{\mathcal{M}}})$) for MUEs are given

This article has been accepted for publication in a future issue of this journal, but has not been fully edited. Content may change prior to final publication. Citation information: DOI 10.1109/TVT.2021.3076825, IEEE Transactions on Vehicular Technology

$$\mathbb{L}(\boldsymbol{\Lambda}, \boldsymbol{P_{\mathcal{M}}}, t, \delta^{\mathcal{M}}, \zeta_m^{\mathcal{M}}) = \sum_{m=1}^{\mathcal{M}} \sum_{r=1}^{\mathcal{R}} \Lambda_{m,B}^r \log_2(1+\gamma_{m,B}^r) - u^* \left\{ \sum_{m=1}^{\mathcal{M}} \sum_{r=1}^{\mathcal{R}} \Lambda_{m,B}^r P_{m,B}^r \right\} - \delta^{\mathcal{M}} \left\{ P_B^{max} - \sum_{m=1}^{\mathcal{M}} \sum_{r=1}^{\mathcal{R}} \Lambda_{m,B}^r P_{m,B}^r \right\} - \sum_{m=1}^{\mathcal{M}} \sum_{r=1}^{\mathcal{R}} \eta_m^{\mathcal{M}} \left\{ \Lambda_{m,B}^r \log_2(1+\gamma_{m,B}^r) - R_{min} \right\}, \tag{27}$$

in **Algorithm 1**. According to **Theorem 1**, for a given u and resource allocation policy $(\boldsymbol{\Lambda}, \boldsymbol{P_{\mathcal{M}}})$, we can iteratively obtain the solution of u^*. The process is repeated until the EE is maximized, i.e., $R_T(\boldsymbol{\Lambda}, \boldsymbol{P_{\mathcal{M}}}) - q(.)P_T(\boldsymbol{\Lambda}, \boldsymbol{P_{\mathcal{M}}}) \leq \epsilon$, where $u(.) = \frac{R_T(\boldsymbol{\Lambda}, \boldsymbol{P_{\mathcal{M}}})}{P_T(\boldsymbol{\Lambda}, \boldsymbol{P_{\mathcal{M}}})}$ is the EE at the iteration (.) and ϵ is a small-valued maximum tolerance level.

Algorithm 1: Resource allocation policy $(\boldsymbol{\Lambda}, \boldsymbol{P_{\mathcal{M}}})$ for MUEs

1 **Initialization:** $t = 0$ and $u(t) = 0$;
2 Set maximum number of iterations t_{max} and maximum tolerance level ϵ;
3 Initialize Lagrange multipliers $\delta^{\mathcal{M}}, \zeta^{\mathcal{M}}$ and step size ξ_1, ξ_2 ;
4 **Iteration:**;
5 **while** *not converged OR* $t! = t_{max}$ **do**
6 Obtain resource allocation policies $(\boldsymbol{\Lambda}', \boldsymbol{P}'_{\boldsymbol{\mathcal{M}}})$;
7 Given $u(t)$, loop over MUE m ;
8 **while** $m! = \mathcal{M}$ **do**
9 Obtain $P_{m,B}^r$ using equation (28). ;
10 Obtain $\Lambda_{m,B}^r$ using equation (30). ;
11 Update $\delta^{\mathcal{M}}, \zeta^{\mathcal{M}}$ using equations (31) and (32).;
12 **end**
13 **if** $R_T(\boldsymbol{\Lambda}', \boldsymbol{P}'_{\boldsymbol{\mathcal{M}}}) - u(t)P_T(\boldsymbol{\Lambda}', \boldsymbol{P}'_{\boldsymbol{\mathcal{M}}}) \leq \epsilon$ **then**
14 converge=true;
15 Set $(\boldsymbol{\Lambda}^*, \boldsymbol{P}^*_{\boldsymbol{\mathcal{M}}}) = (\boldsymbol{\Lambda}', \boldsymbol{P}'_{\boldsymbol{\mathcal{M}}})$
16 **end**
17 **else**
18 converge=false;
19 Set $u(t+1) = \frac{R_T(\boldsymbol{\Lambda}', \boldsymbol{P}'_{\boldsymbol{\mathcal{M}}})}{P_T(\boldsymbol{\Lambda}', \boldsymbol{P}'_{\boldsymbol{\mathcal{M}}})}$;
20 Set t=t+1 ;
21 **end**
22 **end**

B. Resource Allocation Policy for Small Cells

As small cell users reuse the macro cell user RBs, the RB scheduling policy for small cell users must satisfy the constraints $\vec{C2}$, $\vec{C3}$, $\vec{C6}$ and $\vec{C7}$. The constraint $\vec{C2}$ enforces that each macro cell user RB can be utilized by either the SUE or C-IoT device. The underlaid approach of RB selection for SUEs and C-IoTs must satisfy the QoS requirements of the MUEs (i.e., $\vec{C6}$) and fronthaul capacity constraint of H-CRAN (i.e., $\vec{C7}$). Assuming a fixed power allocation in each small cell, **Algorithm 2** iteratively verifies the constraints $\vec{C2}$ and $\vec{C3}$ that each MUE RB is associated with only one SUE or C-IoT device in each small cell (Line 6 and 14). If the constraints $\vec{C2}$ and $\vec{C3}$ are satisfied, then the MUE minimum data rate constraint $\vec{C6}$ is verified in line 8 and line 16 for the SUE and the C-IoT device, respectively. The fronthaul capacity constraint $\vec{C7}$ is verified in line 21. The **Algorithm 2** verifies all the constraints of **P4** and returns the underlaid approach of RB allocation of the SUEs and C-IoT devices. Using this RB allocation solution, we apply the Alternating Direction Method of Multipliers (ADMM) [20], [21] to update the power allocation in each small cell. Using the ADMM method, we can solve the power allocation problem of **P4** in a distributed manner. Each RRH j applies an ADMM based power update policy (i.e., **Algorithm 3**) for the SUE and the C-IoT device. Utilizing ADMM method, the power allocation problem of SUE and C-IoT devices for RRH j can be defined as follows:

$$\text{P5:} \min_{\boldsymbol{\Gamma}, \boldsymbol{\Theta}, \boldsymbol{P_{\mathcal{I}}}, \boldsymbol{P_{\mathcal{D}}}} f(\boldsymbol{\Gamma}, \boldsymbol{P_{\mathcal{I}}}) + g(\boldsymbol{\Theta}, \boldsymbol{P_{\mathcal{D}}}) \tag{33}$$
$$\sum_{i=1}^{\mathcal{I}} \sum_{r=1}^{\mathcal{R}} \mathcal{P}_{\mathcal{I}}{}_{i,j}^r + \sum_{d=1}^{\mathcal{D}} \sum_{r=1}^{\mathcal{R}} \mathcal{P}_{\mathcal{D}}{}_{d,j}^r \leq P_j^{max}$$

where

$$f(\boldsymbol{\Gamma}, \boldsymbol{P_{\mathcal{I}}}) = \sum_{i=1}^{\mathcal{I}} \sum_{r=1}^{\mathcal{R}} \Gamma_{i,j}^r R_{i,j}^r - v_j^1 \left(\sum_{i=1}^{\mathcal{I}} \sum_{r=1}^{\mathcal{R}} \Gamma_{i,j}^r P_{i,j}^r + P_j \right)$$

$$g(\boldsymbol{\Theta}, \boldsymbol{P_{\mathcal{D}}}) = \sum_{i=1}^{\mathcal{D}} \sum_{r=1}^{\mathcal{R}} \Theta_{d,j}^r R_{d,j}^r - v_j^2 \left(\sum_{d=1}^{\mathcal{D}} \sum_{r=1}^{\mathcal{R}} \Theta_{d,j}^r P_{d,j}^r + \sum_{d=1}^{\mathcal{D}} P_d \right)$$

$$\mathbb{L}_j(\boldsymbol{\Gamma}, \boldsymbol{P_{\mathcal{I}}}, \boldsymbol{\Theta}, \boldsymbol{P_{\mathcal{D}}}, \chi_j) = \sum_{i=1}^{\mathcal{I}} \sum_{r=1}^{\mathcal{R}} \Gamma_{i,j}^r R_{i,j}^r - v_j^1 \left(\sum_{i=1}^{\mathcal{I}} \sum_{r=1}^{\mathcal{R}} \Gamma_{i,j}^r P_{i,j}^r + P_j \right) + \sum_{i=1}^{\mathcal{D}} \sum_{r=1}^{\mathcal{R}} \Theta_{d,j}^r R_{d,j}^r - v_j^2 \left(\sum_{d=1}^{\mathcal{D}} \sum_{r=1}^{\mathcal{R}} \Theta_{d,j}^r P_{d,j}^r + \sum_{d=1}^{\mathcal{D}} P_d \right) - \chi_j \left\{ P_j^{max} - \sum_{i=1}^{\mathcal{I}} \sum_{r=1}^{\mathcal{R}} \Gamma_{i,j}^r P_{i,j}^r - \sum_{d=1}^{\mathcal{D}} \sum_{r=1}^{\mathcal{R}} \Theta_{d,j}^r P_{d,j}^r \right\} - \frac{\rho}{2} \left(P_j^{max} - \sum_{i=1}^{\mathcal{I}} \sum_{r=1}^{\mathcal{R}} \Gamma_{i,j}^r P_{i,j}^r - \sum_{d=1}^{\mathcal{D}} \sum_{r=1}^{\mathcal{R}} \Theta_{d,j}^r P_{d,j}^r \right)^2 \tag{34}$$

variable update:

$$\{\boldsymbol{P_{\mathcal{I}}}\}^{t+1} = \arg\min_{\boldsymbol{P_{\mathcal{I}}}} = \mathbb{L}_j(\boldsymbol{\Gamma}, \boldsymbol{P_{\mathcal{I}}}, \boldsymbol{\Theta}, \{\boldsymbol{P_{\mathcal{D}}}\}^t, \chi_j{}^t)$$

$$\{\boldsymbol{P_{\mathcal{D}}}\}^{t+1} = \arg\min_{\boldsymbol{P_{\mathcal{D}}}} = \mathbb{L}_j(\boldsymbol{\Gamma}, \{\boldsymbol{P_{\mathcal{I}}}\}^{t+1}, \boldsymbol{\Theta}, \boldsymbol{P_{\mathcal{D}}}, \chi_j{}^t)$$

This article has been accepted for publication in a future issue of this journal, but has not been fully edited. Content may change prior to final publication. Citation information: DOI 10.1109/TVT.2021.3076825, IEEE Transactions on Vehicular Technology

$$\chi_j{}^{t+1} = \chi_j{}^{t} - \rho\Bigg(P_j^{max} - (\sum_{i=1}^{\mathcal{I}}\sum_{r=1}^{\mathcal{R}} \Gamma_{i,j}^{r} P_{i,j}^{r})^{t+1} - (\sum_{d=1}^{\mathcal{D}}\sum_{r=1}^{\mathcal{R}} \Theta_{d,j}^{r} P_{d,j}^{r})^{t+1} \Bigg) \quad (35)$$

Algorithm 2: Iterative algorithm for obtaining the underlaid RB allocation policy $(\mathbf{\Gamma}, \boldsymbol{P_{\mathcal{L}}}, \mathbf{\Theta}, \boldsymbol{P_{\mathcal{D}}})$ for small cell users

Initialization: For the j^{th} RRH, collects CSI of its users and initialize the parameters $\mathcal{R}$, $\mathcal{I}$, and $\mathcal{D}$;
Resource allocation policy $(\mathbf{\Lambda}, P_{\mathcal{M}})$ obtain from Algorithm 1;
Each j^{th} RRH counts the total number of user requests and sets a fixed power level $p = \frac{P_j^{max}}{\mathcal{I}+\mathcal{D}}$ for each user so that constraint $\vec{C4}$ is satisfied ;
for $r \leftarrow 1$ *to* $\mathcal{R}$ **do**
  for $i \leftarrow 1$ *to* $\mathcal{I}$ **do**
    if $\Lambda_{m,B}^{r} == 1$ *AND* $\Gamma_{i,j}^{r} == 0$ **then** // Check constraints $\vec{C2}$ and $\vec{C3}$
      Considering SUE i, calculate $\gamma_{m,B}^{r}$ and $I_{m,B}^{r}$ using equations (6) and (7);
      if $\Lambda_{m,B}^{r} R_{m,B}^{r} \geq R_{min}$ **then** // Check constraint $\vec{C6}$
        $\Gamma_{i,j}^{r} \leftarrow 1$;
      end
    end
  end
  for $d \leftarrow 1$ *to* $\mathcal{D}$ **do**
    if $\Lambda_{m,B}^{r} == 1$ *AND* $\Gamma_{i,j}^{r} + \Theta_{d,j}^{r}$==0 **then** // Check constraints $\vec{C2}$ and $\vec{C3}$, Find d where r is not used by SUE
      Considering C-IoT d, calculate $\gamma_{m,B}^{r}$ and $I_{m,B}^{r}$ using equations (6) and (7);
      if $\Lambda_{m,B}^{r} R_{m,B}^{r} \geq R_{min}$ **then** // Check constraint $\vec{C6}$
        $\Theta_{d,j}^{r} \leftarrow 1$;
      end
    end
  end
  if $\sum\sum \Gamma_{i,j}^{r} + \sum\sum \Theta_{d,j}^{r} > P_j^{max}$ **then** // Check constraint $\vec{C7}$
    break;
  end
end
return $(\mathbf{\Gamma}, \boldsymbol{P_{\mathcal{I}}}, \mathbf{\Theta}, \boldsymbol{P_{\mathcal{D}}})$

IV. Simulation Results

In the simulation model, we consider a 120 m × 100 m area, where one macro base station is underlaid by 5 to 6 small cell base stations. The locations of MBS, RRHs and C-IoTs are fixed. The locations of SUEs and MUEs are modeled using a spatial Poisson point process with predefined intensity values. The number of RBs and MUEs are constant and the number of SUEs and C-IoTs are varied from 1 to 200. For small cell users, the distance based pathloss model is considered. Also, we consider the location-aware user association scheme, where the users are associated with the closest base station depending on the relative distance and signal strength. The settings for the simulation parameters are shown in Table II. The simulation

Algorithm 3: Using ADMM method to update the power allocation for each small cell.

Initialization: Initialize the constant parameter P_j^{max},v_j^1,v_j^2, χ_j and set a threshold value ϵ, which is a small positive number ;
Initialize RB and power $(\mathbf{\Gamma}, \boldsymbol{P_{\mathcal{I}}}, \mathbf{\Theta}, \boldsymbol{P_{\mathcal{D}}})^t$ using Algorithm 2;
for $t = 1, 2, ..$ **do** // Using Equations (34)and(35) update power to satisfy the constraint $\vec{C4}$
  Set $\{\boldsymbol{P_{\mathcal{I}}}\}^{t+1} = \arg\min_{\boldsymbol{P_{\mathcal{I}}}} = \mathbb{L}_j(\mathbf{\Gamma}, \boldsymbol{P_{\mathcal{I}}}, \mathbf{\Theta}, \{\boldsymbol{P_{\mathcal{D}}}\}^t, \chi_j{}^t)$;
  Set $\{\boldsymbol{P_{\mathcal{D}}}\}^{t+1} = \arg\min_{\boldsymbol{P_{\mathcal{D}}}} = \mathbb{L}_j(\mathbf{\Gamma}, \{\boldsymbol{P_{\mathcal{I}}}\}^{t+1}, \mathbf{\Theta}, \boldsymbol{P_{\mathcal{D}}}, \chi_j{}^t)$;
  update $\chi_j{}^{t+1}$ using the method (35);
  If the stopping criteria are satisfied, go to step 9 ;
end
return $(\mathbf{\Gamma}, \boldsymbol{P_{\mathcal{I}}}, \mathbf{\Theta}, \boldsymbol{P_{\mathcal{D}}})$

TABLE II: Simulation parameters

Parameters	Values
Total number of H-CRAN small cell users (SUEs & C-IoTs)	$1 - 200$
Total number of RBs	100
Total number of H-CRAN macro cell users (MUEs)	100
RB bandwidth	180 kHz
System bandwidth	20 MHz
Radius of small cell	10 m
Minimum data rate requirements	10-10^4 bps/Hz
Transmission power of RRH	$10 - 29$ dBm
Transmission power of MBS	$30 - 43$ dBm
Path-loss exponent	4
Path-loss model for macro cell	$128.1 + 37.6\log_{10}(d)$
Path-loss model for small cell	$140.7 + 36.7\log_{10}(d)$
Noise power spectral density	-144 dBm/Hz

runs are averaged over 1000 iterations. The performance of our proposed method is evaluated in terms of EE and Jain's fairness index in H-CRAN. According to the EE of the entire H-CRAN system, we define the Jain's fairness index as:

$$F = \frac{\left(\sum_{j=1}^{\mathcal{J}} \eta_j\right)^2}{\mathcal{J}\sum_{j=1}^{\mathcal{J}} \eta_j^2}. \quad (36)$$

The performance of the proposed solution of underlaid C-IoT supported H-CRAN (i.e., **Algorithm 1**, **Algorithm 2** and **Algorithm 3**) is compared against that of two baseline schemes using two different power budgets of macro and small cell base stations.

- Baseline one - Overlaid C-IoT supported H-CRAN (OC-IoT): To avoid intra-tier interference, the H-CRAN allocates the orthogonal RBs to all MUEs, SUEs and C-IoTs in a sequential order. At first, all MUEs choose the RBs based on the minimum data rate requirements (i.e., constraint C6). Then, the rest of the RBs are equally allocated to all small cells. For power control, all base stations cooperatively optimize the transmit power to maximize the EE of the H-CRAN system.
- Baseline two - Underlaid H-CRAN without C-IoT (U) [9]: All the RBs of MUEs are shared by the SUEs. The optimal power and RB allocation to maximize the sum of the tolerable interference levels in H-CRAN are considered as in [9]. The number of users, small cell base

This article has been accepted for publication in a future issue of this journal, but has not been fully edited. Content may change prior to final publication. Citation information: DOI 10.1109/TVT.2021.3076825, IEEE Transactions on Vehicular Technology

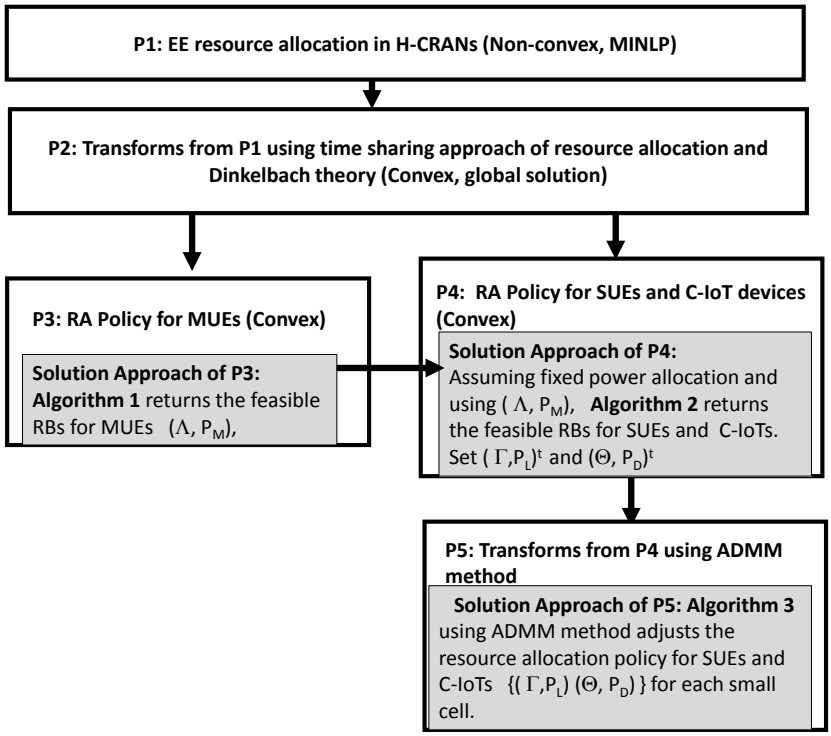

Fig. 3: Problem transformations and energy efficient underlaid C-IoT supported H-CRAN (UC-IoT) solution method.

stations and their location are the same as in baseline one.

- Proposed scheme - Underlaid C-IoT supported H-CRAN (UC-IoT): The UC-IoT method sequentially applies the three algorithms to obtain the underlaid EE solution for H-CRAN. The sequential flow of problem transformations and solution approaches is shown in Fig. 3. In the UC-IoT method, initially **Algorithm 1** is applied to obtain the EE solution for MUEs. Then, **Algorithm 2** is applied which considers an equal power allocation and utilizes the MUE RBs to find the feasible RBs for SUEs and C-IoTs. Lastly, **Algorithm 3** is applied to adjust the EE solution for each small cell in a distributed manner. The number of users, RBs, small cells and locations are the same as in the baseline one. To verify the underlaid approach of RB allocation, the total number of RBs and MUEs are the same and are kept constant.

In the proposed underlaid C-IoT (UC-IoT) method, we utilize Dinkelbach method in **Algorithm 1** to obtain the EE solution for MUEs. The orthogonal multiple access based geometric water filling (OMA-GWF) and branch-and-bound (OMA-BB) algorithms are considered for comparison where each MUE utilizes the orthogonal RB to avoid intra-cell interference [22], [23]. Fig. 4 shows the comparison result among these three algorithms. The upper limit of MBS power (i.e. P_B^{max} = 30dBm) is considered as the water level and the inverse relationship of distance between MUEs and MBS is considered as step depth in the GWF method [22]. In the branch-and-bound method, the total number of branches is equal to the total number of MUEs. For each branch, the boundary is set according to total power (C5) and minimum data rate (C6) constraints. It is shown that the OMA-GWF method and

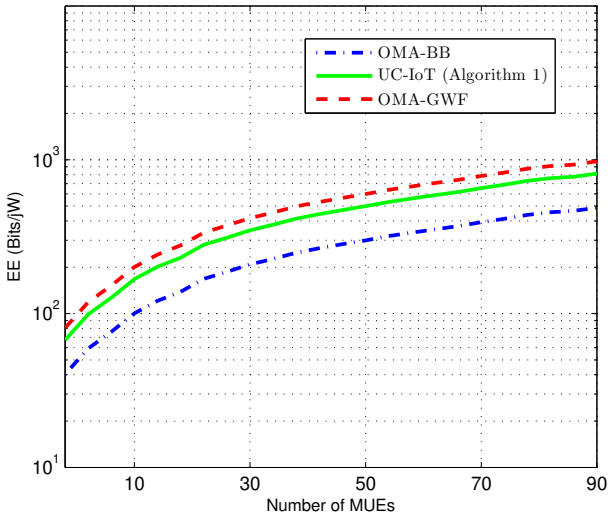

Fig. 4: EE performance comparison of Algorithm 1 (Dinkelbach) with Geometric water filling (GWF) and branch-and-bound (BB) algorithms when the upper limit of macro base station power is $P_B^{max} = 30dBm$.

Algorithm 1 return the most optimized EE performance of MUEs. The OMA-GWF performs better than **Algorithm 1** because it allocates more power to the closest proximity MUEs and that increases the total data rate of the macro cell in H-CRAN system. On the other hand, **Algorithm 1** iteratively optimizes the total power depending on the optimal setting of the Lagrange multipliers, step size values and maximum tolerance level. The OMA-BB method shows the least EE

This article has been accepted for publication in a future issue of this journal, but has not been fully edited. Content may change prior to final publication. Citation information: DOI 10.1109/TVT.2021.3076825, IEEE Transactions on Vehicular Technology

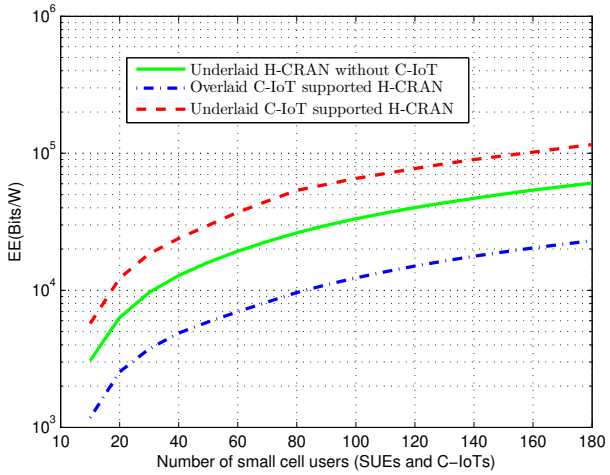

Fig. 5: EE performance of H-CRAN with different number of small cell users.

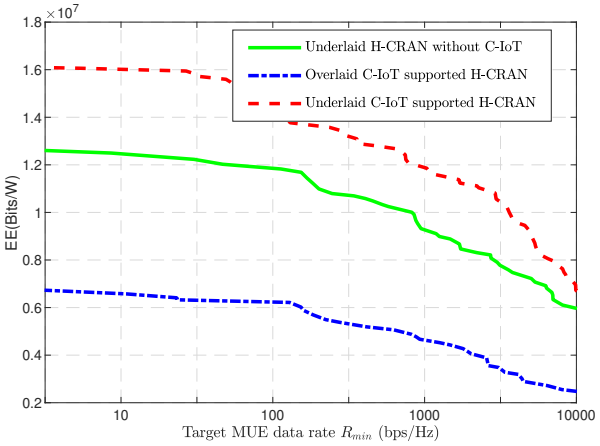

Fig. 6: EE performance of H-CRAN with different minimum rate requirements of MUEs.

performance due to the imposed constraints C5, C6 in the BB method.

The EE performance of the UC-IoT method is compared against that of the overlaid with C-IoT (OC-IoT) and underlaid without C-IoT (U) method as shown in Figs. 5 and 6 respectively, where we have considered one MBS that consumes maximum 43 dBm power and each RRH has 29 dBm maximum power budget [8]. In the UC-IoT method, the **Algorithm 1** allocates the power to the RB during the resource allocation to MUE. **Algorithm 2** considers equal power levels for the RBs to find the feasible RB lists for the SUEs and C-IoTs so that the data rates of the MUEs are not changed. Lastly, **Algorithm 3** optimizes each RRH power to provide the EE solution in H-CRAN. Similarly, the underlaid approach of resource allocation in H-CRAN is considered in [9], where an underlaid H-CRAN is considered without C-IoT system, with the objective to maximize the tolerable interference level so that the SUEs and MUEs can share the same RBs without violating the QoS constraints of

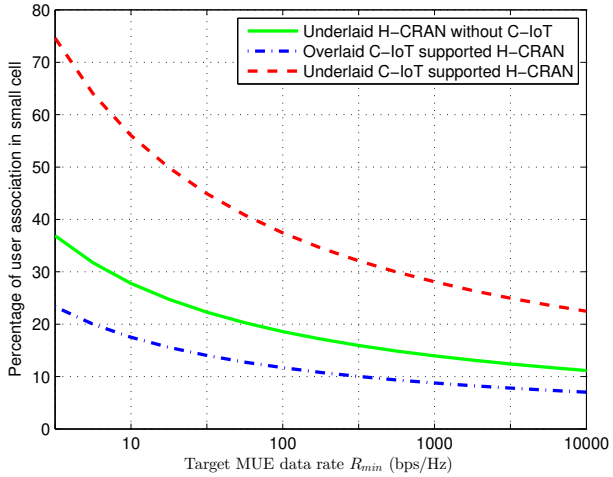

Fig. 7: Impact of different minimum rate requirements of MUEs to the percentage of user association in small cell of H-CRAN.

the MUEs and SUEs. The difference between UC-IoT and U-method is that the U-method considers both the SUE's and MUE's data rate requirements. Maintaining these two requirements and underlaid approach of RB allocation, the U-method restricts fewer number of SUEs to be admitted to the system than the UC-IoT method. On the other hand, the UC-IoT method relaxes the SUE's data rate requirement, considers the MUEs as legacy users, and maintains the minimum data rate requirement of these users in finding a solution for the RB allocation for the SUEs and C-IoTs.

Fig. 6 and Fig. 7 show a comparison of the EE performance and user association percentage of H-CRAN using these methods in terms of different minimum data rate requirements of the MUEs. It is shown that the underlaid approach of resource (i.e., RBs and power) allocation methods (i.e., UC-IoT and U) are always better than the overlaid method (OC-IoT). This can be explained by each user using orthogonal RBs to avoid interference in the OC-IoT method. The total number of user association depends on the total number of RBs available in the system. Due to the limited number of RBs, the user association percentage and the sum data rate of the OC-IoT method is less than that obtained for the UC-IoT method, which reduces the EE of the H-CRAN since EE is estimated as the ratio of the sum data rate to the total allocated power to the RBs.

The sum data rate and convergence behavior of the UC-IoT method are investigated with three different power budgets; i) $P_j^{max} = 10$ dBm, $P_B^{max} = 30$dBm, ii)$P_j^{max} = 15$ dBm, $P_B^{max} = 35$dBm, and iii) $P_j^{max} = 29$dBm, $P_B^{max} = 43$dBm. Fig. 8 shows the performance of the sum data rate performance of the UC-IoT method for the C-IoT density in each small cell. It can be observed that the sum data rate performance of the UC-IoT method gives better results when more power is used for RRHs and MBS. This is due to the fact that in the location based user association, the user i connects to the base station j based on the maximum received channel state information

This article has been accepted for publication in a future issue of this journal, but has not been fully edited. Content may change prior to final publication. Citation information: DOI 10.1109/TVT.2021.3076825, IEEE Transactions on Vehicular Technology

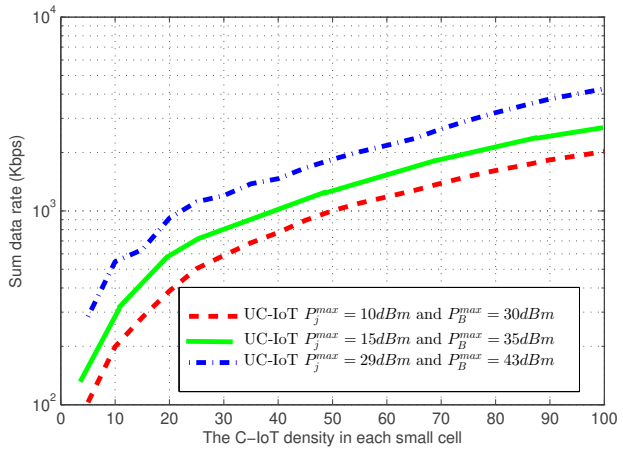

Fig. 8: Sum data rate performance of underlaid C-IoT supported H-CRAN (UC-IoT) with three different power budgets.

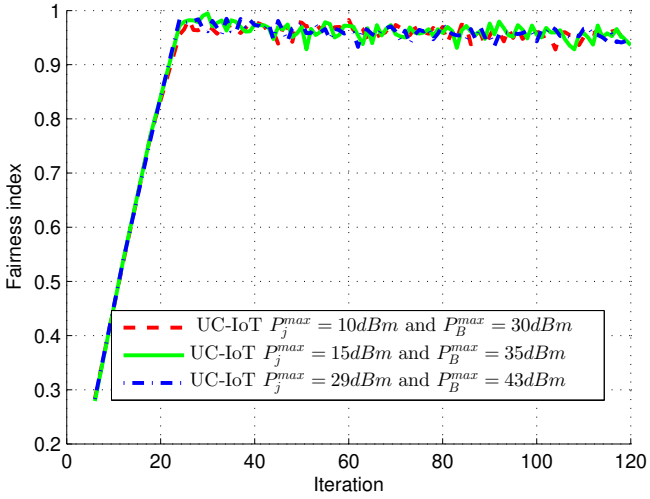

Fig. 9: Convergence behavior of Algorithm 2 and Algorithm 3.

(CSI). Considering equal transmission power in each small cell and the noise factor, according to the distance dependent pathloss model, the SINR of each user becomes maximum when the distance between the user and base station becomes minimum.

Similar to [24] and [25], the convergence behavior of **Algorithm** 2 and **Algorithm** 3 is shown with the fairness index versus iteration number in Fig. 9. We consider C-IoT density in each small cell to be 50. Using the results of **Algorithm** 1 and equal power budget for each RRH, we apply **Algorithm** 2 and **Algorithm** 3 to find the EE solution of each RRH. According to the definition of the Jain's index in (36), a higher value of J represents a fair allocation of resources in H-CRAN in the perspective of EE solution for each small cell (i.e., RRH). It is apparent from Fig. 9 that the EE solution for RRHs (i.e., **Algorithm** 2 and **Algorithm** 3) for different power budgets shows non-decreasing EE and convergence within a fair resource allocation within 20 to 40 iterations.

V. Conclusion

In this paper, we proposed an energy efficient underlaid resource allocation method for two-tier OFDMA-based cellular IoT supported H-CRAN systems, where users in a small cell uses the same radio resources with the macro cell in an underlaid approach. The proposed underlaid C-IoT supported H-CRAN (UC-IoT) resource allocation method (i.e., **Algorithm** 1, **Algorithm** 2 and **Algorithm** 3) have been shown to satisfy the resource allocation and maximum power constraints for both macro and small cell base stations, as well as the interference, fronthaul capacity and QoS constraints of macro cell users. Simulation results have shown that the proposed UC-IoT method converges and also improves the EE in C-IoT supported H-CRAN through the underlaid approach of resource allocation. The tradeoff between EE and throughput in the proposed (UC-IoT) resource allocation method will be considered in a future work.

Appendix

Proof of Theorem 1: Let the feasible solution of (25) be denoted as $(\boldsymbol{\Lambda}, \boldsymbol{P_{\mathcal{M}}})$. Since $(\boldsymbol{\Lambda}^*, \boldsymbol{P^*_{\mathcal{M}}})$ is the optimal solution to the problem,

$$R_T(\boldsymbol{\Lambda}^*, \boldsymbol{P^*_{\mathcal{M}}}) - u^* P_T(\boldsymbol{\Lambda}, \boldsymbol{P_{\mathcal{M}}}) \geq R_T(\boldsymbol{\Lambda}, \boldsymbol{P_{\mathcal{M}}}) - u^* P_T(\boldsymbol{\Lambda}, \boldsymbol{P_{\mathcal{M}}}),$$

and $R_T(\boldsymbol{\Lambda}^*, \boldsymbol{P^*_{\mathcal{M}}}) - u^* P_T(\boldsymbol{\Lambda}, \boldsymbol{P_{\mathcal{M}}}) = 0$, and $R_T(\boldsymbol{\Lambda}, \boldsymbol{P_{\mathcal{M}}}) - u^* P_T(\boldsymbol{\Lambda}, \boldsymbol{P_{\mathcal{M}}}) \leq 0$, where $P_T(\boldsymbol{\Lambda}, \boldsymbol{P_{\mathcal{M}}})$ is the H-CRAN power consumption which is greater than zero. Therefore,

$$\frac{R_T(\boldsymbol{\Lambda}, \boldsymbol{P_{\mathcal{M}}})}{P_T(\boldsymbol{\Lambda}, \boldsymbol{P_{\mathcal{M}}})} \leq u^*.$$

Hence,

$$\frac{R_T(\boldsymbol{\Lambda}, \boldsymbol{P_{\mathcal{M}}})}{P_T(\boldsymbol{\Lambda}, \boldsymbol{P_{\mathcal{M}}})} \leq \frac{R_T(\boldsymbol{\Lambda}^*, \boldsymbol{P^*_{\mathcal{M}}})}{P_T(\boldsymbol{\Lambda}^*, \boldsymbol{P^*_{\mathcal{M}}})}.$$

Thus, $(\boldsymbol{\Lambda}^*, \boldsymbol{P^*_{\mathcal{M}}})$ maximizes

$$\frac{R_T(\boldsymbol{\Lambda}, \boldsymbol{P_{\mathcal{M}}})}{P_T(\boldsymbol{\Lambda}, \boldsymbol{P_{\mathcal{M}}})}$$

while satisfying all the constraints in the relaxed optimization problem **P3**. □

B. Calculation of Power Allocation for MUE

$$\mathbb{L}(\boldsymbol{\Lambda}, \boldsymbol{P_{\mathcal{M}}}, u, \delta^{\mathcal{M}}, \boldsymbol{\eta^{\mathcal{M}}}) = \sum_{m=1}^{\mathcal{M}} \sum_{r=1}^{\mathcal{R}} \Lambda^r_{m,B} \log_2(1 + P^r_{m,B} G^r_{m,B}) - u \left\{ \sum_{m=1}^{\mathcal{M}} \sum_{r=1}^{\mathcal{R}} \Lambda^r_{m,B} P^r_{m,B} \right\} - \delta^{\mathcal{M}} \left\{ P_B^{max} - \sum_{m=1}^{\mathcal{M}} \sum_{r=1}^{\mathcal{R}} \Lambda^r_{m,B} P^r_{m,B} \right\} - \sum_{m=1}^{\mathcal{M}} \sum_{r=1}^{\mathcal{R}} \eta^{\mathcal{M}}_m \left\{ \Lambda^r_{m,B} \log_2(1 + P^r_{m,B} G^r_{m,B}) - R_{min} \right\}, \quad (37)$$

Differentiating (37) with respect to $P^r_{m,B}$, we obtain the following power allocation of MUE m over RB r as

$$\begin{aligned}
&\frac{\partial \mathbb{L}}{\partial P^r_{m,B}} = 0 \\
&\frac{\Lambda^r_{m,B} G^r_{m,B}}{\ln(1+P^r_{m,B}G^r_{m,B})} - u\Lambda^r_{m,B} + \delta^{\mathcal{M}}\Lambda^r_{m,B} - \frac{\eta^{\mathcal{M}}_m \Lambda^r_{m,B} G^r_{m,B}}{\ln(1+P^r_{m,B}G^r_{m,B})} = 0 \\
&\frac{\Lambda^r_{m,B} G^r_{m,B}(1-\eta^{\mathcal{M}}_m)}{\ln(1+P^r_{m,B}G^r_{m,B})} = \Lambda^r_{m,B}(u-\delta^{\mathcal{M}})
\end{aligned} \tag{38}$$

Therefore, $P^r_{m,B}$ can be obtained as

$$P^r_{m,B} = \left[\frac{1-\eta^{\mathcal{M}}_m}{\ln(u-\delta^{\mathcal{M}})} - \frac{1}{G^r_{m,B}}\right]^+.$$

REFERENCES

[1] A. Checko, H. L. Christiansen, Y. Yan, L. Scolari, G. Kardaras, M. S. Berger, and L. Dittmann, "Cloud-RAN for mobile networks - a technology overview," *IEEE Commun. Surveys Tut.*, vol. 17, pp. 405 – 426, Sep. 2015.

[2] L. Ferdouse, A. Anpalagan, and S. Erkucuk, "Joint communication and computing resource allocation in 5g cloud radio access networks," *IEEE Trans. Vehic. Techno.*, vol. 68, pp. 9122–9135, Sep. 2019.

[3] X. Zhang, M. Jia, X. Gu, and Q. Guo, "An energy efficient resource allocation scheme based on cloud-computing in H-CRAN," *IEEE Internet of Things Journal*, vol. 6, pp. 4968–4976, June 2019.

[4] S. Dama, V. Sathya, K. Kuchi, and T. V. Pasca, "A feasible cellular internet of things: Enabling edge computing and the iot in dense futuristic cellular networks," *IEEE Consumer Elect Mag*, vol. 6, pp. 66–72, Jan 2017.

[5] B. Alzahrani and W. Ejaz, "Resource management for cognitive IoT systems with RF energy harvesting in smart cities," *IEEE Access*, vol. 6, pp. 62717–62727, 2018.

[6] T. Salam, W. U. Rehman, and X. Tao, "Data aggregation in massive machine type communication: challenges and solutions," *IEEE Access*, vol. 7, pp. 41921–41946, 2019.

[7] D. Wubben, P. Rost, J. S. Bartelt, M. Lalam, V. Savin, M. Gorgoglione, A. Dekorsy, and G. Fettweis, "Benefits and impact of cloud computing on 5g signal processing: Flexible centralization through cloud-RAN," *IEEE Signal Process. Mag.*, vol. 31, pp. 35 – 44, Oct. 2014.

[8] Q. Liu, T. Han, N. Ansari, and G. Wu, "On designing energy-efficient heterogeneous cloud radio access networks," *IEEE Trans. Green Commun. Net.*, vol. 2, pp. 721–734, Sep. 2018.

[9] A. Abdelnasser and E. Hossain, "Resource allocation for an OFDMA Cloud-RAN of small cells underlaying a macrocell," *IEEE Trans. Mobile Comput.*, vol. 15, pp. 2837–2850, Nov. 2016.

[10] A. Alnoman and A. S. Anpalagan, "Computing-aware base station sleeping mechanism in h-cran-cloud-edge networks," *IEEE Transactions on Cloud Computing*, pp. 1–1, 2019.

[11] N. A. Chughtai, M. Ali, S. Qaisar, M. Imran, M. Naeem, and F. Qamar, "Energy efficient resource allocation for energy harvesting aided h-cran," *IEEE Access*, vol. 6, pp. 43990–44001, 2018.

[12] N. Amani, H. Pedram, H. Taheri, and S. Parsaeefard, "Energy-efficient resource allocation in heterogeneous cloud radio access networks via BBU offloading," *IEEE Trans. Vehic. Tech.*, vol. 68, pp. 1365–1377, Feb. 2019.

[13] L. Ferdouse, O. Das, and A. Anpalagan, "Auction based distributed resource allocation for delay aware OFDM based Cloud-RAN system," in *IEEE Global Commun. Conf.*, pp. 1–6, Dec. 2017.

[14] B. Xu, Y. Chen, J. R. Carrion, and T. Zhang, "Resource allocation in energy-cooperation enabled two-tier NOMA HetNets toward green 5G," *IEEE Journ. Select. Areas Commun.*, vol. 35, pp. 2758–2770, Dec. 2017.

[15] Q. Liu, T. Han, N. Ansari, and G. Wu, "On designing energy-efficient heterogeneous cloud radio access networks," *IEEE Trans. Green Commun. Net.*, vol. 2, pp. 721–734, Sep. 2018.

[16] Z. Chang, Z. Wang, X. Guo, C. Yang, Z. Han, and T. Ristaniemi, "Distributed resource allocation for energy efficiency in OFDMA multicell networks with wireless power transfer," *IEEE Journ. Select. Areas Commun.*, vol. 37, pp. 345–356, Feb. 2019.

[17] M. Hasan and E. Hossain, "Resource allocation for network-integrated device-to-device communications using smart relays," in *2013 IEEE Globecom Workshops (GC Wkshps)*, pp. 591–596, Dec. 2013.

[18] E. H. Monowar Hasan and D. I. Kim, "Resource Allocation Under Channel Uncertainties for Relay-Aided Device-to-Device Communication Underlaying LTE-A Cellular Networks," *IEEE Trans. Wire. commun.*, vol. 13, pp. 2322–2338, Mar. 2014.

[19] W. Yu and R. Lui, "Dual methods for nonconvex spectrum optimization of multicarrier systems," *IEEE Trans. Commun.*, vol. 54, pp. 1310–1322, July 2006.

[20] D. Gabay and B. Mercier, "A dual algorithm for the solution of nonlinear variational problems via finite element approximations," *Computers and Mathematics with Applications*, vol. 2, no. 1, pp. 17–40, 1976.

[21] J.Eckstein, "Augmented lagrangian and alternating direction methods for convex optimization: a tutorial and some illustrative computational results," *Rutgers Univ., New Brunswick,NJ,USA, RUTCOR Res. Rep.*, 2012.

[22] P. He, L. Zhao, S. Zhou, and Z. Niu, "Water-filling: A geometric approach and its application to solve generalized radio resource allocation problems," *IEEE Trans. on Wire. Commun.*, vol. 12, no. 7, pp. 3637–3647, 2013.

[23] I. Quesada and I. Grossmann, "An LP/NLP based branch and bound algorithm for convex MINLP optimization problems," *Computers and Chemical Eng.*, vol. 16, no. 10, pp. 937 – 94, 1992.

[24] J. V. C. Evangelista, Z. Sattar, G. Kaddoum, and A. Chaaban, "Fairness and sum-rate maximization via joint subcarrier and power allocation in uplink scma transmission," *IEEE Transactions on Wireless Communications*, vol. 18, no. 12, pp. 5855–5867, 2019.

[25] D. C. R. Jain and W. Hawe, "A quantitative measure of fairness and discrimination for resource allocation in shared systems," in *Digital Equipment Corporation, Tech. Rep. DEC-TR-301*, Sep 1984.

Lilatul Ferdouse received the M.A.Sc. degree in Electrical and Computer Engineering from Ryerson University, Toronto, ON, Canada, in 2015, and the Ph.D degree from Ryerson University in 2019. Currently, she is postdoctoral research fellow with the WINCORE and DABNEL labs. Her research interests are in resource allocation of next generation wireless communication systems, relay assisted cooperative networks, congestion, and overload control techniques in M2M and IoT networks..

Isaac Woungang received his Ph.D. degree in Mathematics from University of South, Toulon and Var, France, in 1994. From 1999 to 2002, he worked as Senior Software Engineer at Nortel Networks, Ottawa, Canada. Since 2002, he has been with Ryerson University, where he is now a Professor of Computer Science and Director of the DABNEL Research Lab. His current research interests include radio resource management in next generation wireless networks, computer security, computational intelligence and machine learning applications, performance modelling, and optimization. He has published 8 edited books, 1 authored books, and over 80 refereed journals and conference papers.

Alagan Anpalagan (S98-M01-SM04) received the B.A.Sc., M.A.Sc., and Ph.D. degrees, all in electrical engineering from the University of Toronto, Canada. He joined with the ELCE Department, Ryerson University, Canada in 2001, and was promoted to Full Professor in 2010. He served the department in administrative positions as Associate Chair, Program Director for Electrical Engineering, and Graduate Program Director. During his sabbatical, he was a Visiting Professor at Asian Institute of Technology, and Visiting Researcher at Kyoto University. His industrial experience includes working for three years with Bell Mobility, Nortel Networks, and IBM. He directs a research group working on radio resource management (RRM) and radio access and networking (RAN) areas within the WINCORE Laboratory. He has coauthored four edited books and two books in wireless communication and networking areas. Dr. Anpalagan served as an Editor for the IEEE COMMUNICATIONS SURVEYS AND TUTORIALS (2012-2014), IEEE COMMUNICATIONS LETTERS (2010-2013), and EURASIP Journal of Wireless Communications and Networking (2004-2009). He also served as Guest Editor for six special issues published in IEEE, IET and ACM. He served as TPC Co-Chair, IEEE VTC Fall 2017, TPC Co–Chair, IEEE INFOCOM'16: Workshop on Green and Sustainable Networking and Computing, IEEE Globecom15: SAC Green Communication and Computing, IEEE PIMRC'11: Cognitive Radio and Spectrum Management. He served as Vice Chair, IEEE SIG on Green and Sustainable Networking and Computing with Cognition and Cooperation (2015–18), IEEE Canada Central Area Chair (2012-2014), IEEE Toronto Section Chair (2006-2007), ComSoc Toronto Chapter Chair (2004-2005), and IEEE Canada Professional Activities Committee Chair (2009-2011). Dr. Anpalagan was the recipient of the IEEE Canada J.M. Ham Outstanding Engineering Educator Award (2018), YSGS Outstanding Contribution to Graduate Education Award (2017), Deans Teaching Award (2011), Faculty Scholastic, Research and Creativity Award thrice from the Ryerson University. He was also the recipient of IEEE M.B. Broughton Central Canada Service Award (2016), Exemplary Editor Award from IEEE ComSoc (2013) and Editor-in-Chief Top10 Choice Award in Transactions on Emerging Telecommunications Technology (2012) and, a coauthor of a paper that received IEEE SPS Young Author Best Paper Award (2015). He is a Registered Professional Engineer in the province of Ontario, Canada and Fellow of the Institution of Engineering and Technology (FIET) and Fellow of the Engineering Institute of Canada (FEIC).

Serhat Erkucuk (S'99–M'08–SM'19) received the B.Sc. degree in electrical engineering from Middle East Technical University, Ankara, Turkey, in 2001, the M.Sc. degree in electrical and computer engineering from Ryerson University, Toronto, ON, Canada, in 2003, and the Ph.D. degree in engineering science from Simon Fraser University, Burnaby, BC, Canada, in 2007. He was an NSERC Postdoctoral Fellow at The University of British Columbia, Vancouver, Canada, in 2008. He then joined Kadir Has University, Istanbul, Turkey, where he is currently a Full Professor. In 2018, he was a Visiting Professor at Ryerson University, where he conducted research on the design of small cells for 5G networks. His research interests are in physical layer design of emerging communication systems, wireless sensor networks, and communication theory. He is a Marie Curie Fellow and a recipient of the Governor's General Gold Medal.